



*Citation for published version:*

Lopardo, L, Cummins, A, Rydevik, A & Kasprzyk-Hordern, B 2017, 'New Analytical Framework for Verification of Biomarkers of Exposure to Chemicals Combining Human Biomonitoring and Water Fingerprinting', *Analytical Chemistry*, vol. 89, no. 13, pp. 7232-7239. <https://doi.org/10.1021/acs.analchem.7b01527>

*DOI:*

[10.1021/acs.analchem.7b01527](https://doi.org/10.1021/acs.analchem.7b01527)

*Publication date:*

2017

*Document Version*

Peer reviewed version

[Link to publication](#)

This document is the Accepted Manuscript version of a Published Work that appeared in final form in 'Analytical Chemistry', copyright © American Chemical Society after peer review and technical editing by the publisher. To access the final edited and published work see <https://doi.org/10.1021/acs.analchem.7b01527>

## University of Bath

### General rights

Copyright and moral rights for the publications made accessible in the public portal are retained by the authors and/or other copyright owners and it is a condition of accessing publications that users recognise and abide by the legal requirements associated with these rights.

### Take down policy

If you believe that this document breaches copyright please contact us providing details, and we will remove access to the work immediately and investigate your claim.

# 1 A new analytical framework for verification of biomarkers of exposure to chemicals 2 combining human biomonitoring and water fingerprinting

3 Luigi Lopardo, Andrew Cummins, Axel Rydevik and Barbara Kasprzyk-Hordern\*

4 Department of Chemistry, University of Bath, Bath BA2 7AY, UK

## 5 6 Abstract

7 Molecular epidemiology approaches in human biomonitoring are powerful tools that allow for  
8 verification of public exposure to chemical substances. Unfortunately, due to logistical difficulties and  
9 high cost, they tend to evaluate small study groups and as a result might not provide comprehensive  
10 large scale community-wide exposure data. Urban water fingerprinting provides a timely alternative to  
11 traditional approaches. It can revolutionise the human exposure studies as urban water represents  
12 collective community-wide exposure. Knowledge of characteristic biomarkers of exposure to specific  
13 chemicals is key to the successful application of water fingerprinting. This study aims to introduce a  
14 novel conceptual analytical framework for identification of biomarkers of public exposure to chemicals  
15 via combined human metabolism and urban water fingerprinting assay. This framework consists of:  
16 Step 1 - In vitro HLM/S9 assay; Step 2 – In vivo pooled urine assay; Step 3 - In vivo wastewater  
17 fingerprinting assay; Step 4 - Analysis with HR-MSMS; Step 5 - Data processing and Step 6 - Selection  
18 of biomarkers. The framework was applied and validated for PCMC (4-chloro-m-cresol), household  
19 derived antimicrobial agent with no known exposure and human metabolism data. Four new metabolites  
20 of PCMC (hydroxylated, sulphated/hydroxylated, sulphated PCMC and PCMC glucuronide) were  
21 identified using the in vitro HLM/S9 assay. But only one metabolite, sulphated PCMC, was confirmed  
22 in wastewater and in urine. Therefore, our study confirms that water fingerprinting is a promising tool  
23 for biomarker selection and that *in vitro* HLM/S9 studies alone, although informative, do not provide  
24 high accuracy results. Our work also confirms, for the first time, human internal exposure to PCMC.

## 25 26 Introduction

27 Antimicrobials are extensively used as additives in a broad range of personal care and consumer  
28 products to preserve the integrity of the products against biological agents, although their effectiveness  
29 against the potential hazard has been questioned<sup>1</sup>. In particular, antimicrobials are added to soaps,  
30 cosmetics and disinfectants to protect against the growth of microorganisms, including bacteria, viruses  
31 and fungi. Some of these chemicals, their metabolites and/or their degradation products have been  
32 reported to be potentially bioaccumulative<sup>2</sup>, endocrine disrupting<sup>3</sup>, ecotoxic in aquatic ecosystems<sup>4</sup> and  
33 leading to microbial resistance<sup>5,6</sup>. However very little is known about actual human exposure to  
34 antimicrobials in personal care products and therefore about the possibility to cause long term health  
35 effects. Even though available information concerning the percutaneous absorption of antimicrobials in  
36 humans is still scarce, it is known that some of them can be absorbed through the skin<sup>7</sup>, suggesting that  
37 exposure results mostly from topical application of personal care products. However, ingestion of  
38 contaminated food and water<sup>8,9</sup> and inhalation of indoor dust<sup>10</sup> represent other important  
39 indirect/environmental sources of exposure. Antimicrobials can be metabolised in humans followed by  
40 excretion of parent compound and their metabolites primarily with urine. Because the presence of those  
41 compounds in blood, serum and urine has been demonstrated<sup>11-15</sup> and their environmental persistence  
42 and widespread use documented, it is unsurprising that they can be found in wastewater and in the  
43 receiving environment<sup>16,17</sup>. Their omnipresence, potential for bioaccumulation and possible synergistic  
44 effects of mixtures have raised public concern regarding their possible effects on human health as well  
45 as their role in the development of antimicrobial resistance<sup>18</sup>. There is therefore the need to consider a  
46 greater range of factors contributing to potential health effects of combined exposures within the risk  
47 assessment process. Risk assessment of mixtures is known to be difficult due to complexity of  
48 contributing factors when compared to the assessment of single chemicals<sup>19</sup>. New approaches towards

---

\* Corresponding author: E-mail: [b.kasprzyk-hordern@bath.ac.uk](mailto:b.kasprzyk-hordern@bath.ac.uk); Fax: +44(0) 1225 386231; Tel: +44 (0) 1225 385013

49 risk assessment and evaluation of public exposure to antimicrobial agents in personal care products are  
50 therefore critically needed.

51 By comparing community levels of environmental stressors (both external and internal) with observed  
52 health effects, conclusions could be drawn as to whether elevated levels of certain chemicals could be  
53 linked with particular diseases. Such epidemiological studies are currently being undertaken via  
54 traditional approaches which use simple tools including case histories, questionnaires, or molecular  
55 epidemiology, which combines the above with sensitive laboratory techniques. These approaches  
56 monitor biological responses, rather than diseases in human populations through the usage of  
57 biomarkers<sup>20</sup>. However, a limitation of molecular epidemiology, due to logistical difficulties and high  
58 cost, is the restricted size of study groups and inability to gather comprehensive information on the  
59 complexity of combined (and cumulative) exposure to mixtures of chemicals and their effects.  
60 Therefore the community lacks robust measures that can be used to gather real-time information on  
61 community-wide health.

62 Urban water fingerprinting for human metabolic biomarkers is a new approach in epidemiological  
63 exposure studies that can revolutionise the way we estimate public exposure to chemicals. This  
64 approach is also known wastewater based epidemiology (WBE). WBE is a new concept that aims to  
65 overcome the above limitations and to provide spatial and temporal near-real time estimation of  
66 community-wide exposure to wide range of chemicals. This unique approach assumes that  
67 epidemiological information can be retrieved from wastewater via the analysis of human metabolic  
68 biomarkers. Although still in its infancy, it is currently used to determine illicit drug use trends at the  
69 community level through the analysis of urinary biomarkers in wastewater<sup>21-23</sup>. This approach can be  
70 also extended to make a real time assessment of population health status<sup>24</sup>. WBE postulates that specific  
71 human metabolic biomarkers (e.g. characteristic metabolites of toxicants or pollutants) excreted with  
72 urine and faeces, and resulting from exposure to certain chemicals, are pooled by the urban wastewater  
73 system providing evidence of the amount and type of toxicants or pollutants to which a population  
74 contributing to the analysed water, has been exposed. Urban water fingerprinting can therefore provide  
75 anonymous and comprehensive estimation of the community-wide health status in near-real time.

76 The selection of unique metabolic biomarkers that are characteristic for each individual chemical and  
77 route of exposure is a critical step in order to verify public exposure to these chemicals via WBE, e.g.  
78 in order to distinguish between internal and external exposure, and to account for direct disposal, since  
79 many sources contribute to chemicals being discharged into wastewater. Unfortunately, in the case of  
80 many chemicals, especially those that are not intended for human consumption (e.g. antimicrobials),  
81 there is no public knowledge of characteristic metabolic biomarkers that could be utilised in WBE.  
82 Nevertheless, due to their extensive use in personal care and consumer products<sup>25</sup> dermal absorption is  
83 considered to be one of the main routes of human exposure. Understanding toxicokinetic process,  
84 including metabolism, is therefore crucial in the determination of toxicological effects and potential for  
85 bioaccumulation of these chemicals, as well as in the identification of biomarkers of exposure. Still,  
86 there are only a few studies which reported their *in vivo* or *in vitro* biotransformation. Wu, Liu and Cai  
87 (2010)<sup>15</sup> investigated the metabolism of triclosan *in vivo* and *in vitro*. They observed both oxidative and  
88 phase II metabolites and identified glucuronidated triclosan as the major metabolite. Schebb et al.  
89 (2011)<sup>25</sup> reported that the 0.6% circa of the amount of triclocarban present in bar soaps ( $70 \pm 15$  mg)  
90 was absorbed through the skin and that the 25% of total amount was excreted in urine almost exclusively  
91 as N-glucuronides. Unfortunately, most antimicrobials still remain hardly investigated.

92 We are proposing a novel conceptual framework for identification of metabolic biomarkers via  
93 combined human metabolism and urban water fingerprinting assays. In this study, we identified, for the  
94 first time, human specific metabolites of the antimicrobial agent, 4-chloro-3-methylphenol (PCMC), as  
95 potential biomarkers of community-wide exposure to PCMC via WBE. This antimicrobial agent, also  
96 known as 4-chloro-*m*-cresol, is a phenolic compound that has been proven to have an estrogenic activity  
97 determined by an *in vitro* yeast bioassay<sup>26</sup>. PCMC is also known to have an effect on Ca<sup>2+</sup> homeostasis  
98 being a strong activator of the ryanodine receptors in the endoplasmic reticulum<sup>27</sup> and to interfere with  
99 the thyroid hormone functions<sup>28</sup>. To the authors' knowledge, there is no published data on metabolic  
100 pathways of PCMC in humans.

## 101 **Experimental section**

### 102 ***Reagents and analytical standards***

103 Pooled human liver microsomes (HLM), S9 fraction pooled from human liver,  $\beta$ -nicotinamide adenine  
104 dinucleotide 2'-phosphate reduced ( $\beta$ -NADPH  $\geq$  95%), Uridine 5'-diphosphoglucuronic acid trisodium  
105 salt (UDPGA 98-100%), alamethicin from *Trichoderma viride* ( $\geq$  98%), 3'-phosphoadenosine 5'-  
106 phosphosulphate lithium salt (PAPS  $\geq$  60%), 4-chloro-3-methylphenol (p-chlorocresol), potassium  
107 phosphate monobasic tetrasodium salt hydrate ( $\text{KH}_2\text{PO}_4$ ), magnesium chloride hexahydrate ( $\text{MgCl}_2$ ),  
108 were purchased from Sigma-Aldrich (Gilligam,UK). The internal standard: 4-chloro-3-methylphenol-  
109 2,6-d2, was purchased from QMX Laboratories Ltd.

110 Solvents were of HPLC purity and were purchased from Sigma-Aldrich (Gilligam, UK). Stock standard  
111 solutions were prepared in methanol and stored in the dark at  $-20^\circ\text{C}$ . 24h volume-proportional (100 mL  
112 every 15 minutes) composite wastewater influent samples were collected in PTFE bottles from a local  
113 wastewater treatment plant (WWTP) serving 70000 inhabitants on the 8<sup>th</sup> of June 2015. They were then  
114 transported to the laboratory in cool boxes packed with ice blocks and filtered through GF/F 0.7  $\mu\text{m}$   
115 glass fibre filter (Whatman, UK).

### 116 ***In vitro assays for verification of metabolic profile of PCMC in humans***

117 Two *in vitro* assays were selected in this study: HLM and combined HLM and S9 fraction. Currently  
118 HLM represents the most commonly used *in vitro* model, providing an affordable way to give a good  
119 indication of the cytochrome P450 (CYP) and uridine 5'-diphospho-glucuronosyltransferase (UGT)  
120 metabolic profile<sup>29</sup>. Unfortunately, the absence of other enzymes such as N-acetyltransferase (NAT),  
121 glutathione S-transferase (GST) and sulphotransferase (ST) implies, as a result, an incomplete range of  
122 metabolites being formed. A valid alternative to the use of HLM is the liver S9 fraction which contains  
123 both microsomal and cytosolic fractions (phase I and phase II metabolic enzymes) that lead to the  
124 formation of a range of metabolites giving, as a result, more representative metabolic profile when  
125 compared to HLM only. However, the overall amount of metabolites formed is lower due to lower  
126 enzyme activity in the S9 fraction when compared to microsomes. This might result in minor  
127 metabolites to remain unnoticed<sup>30</sup>. Therefore, in this paper, method development included different  
128 subcellular fractions (HLM and a combination of HLM and S9 fraction).

129 ***In vitro HLM assay for verification of metabolic profile of PCMC.*** 10  $\mu\text{L}$  of a phosphate buffer (50mM  
130  $\text{KH}_2\text{PO}_4$ , pH 7.4, 5mM  $\text{MgCl}_2$ ), 10  $\mu\text{L}$  of analyte solution (50  $\mu\text{M}$ ) were mixed with 10  $\mu\text{L}$  human liver  
131 microsomes spiked with 1  $\mu\text{L}$  of an alamethicin solution 12.5 mg/mL and 10  $\mu\text{L}$  of a 100 $\mu\text{M}$  UDPGA  
132 solution. The reaction was initiated by addition of 10  $\mu\text{L}$  of a 10 mM NADPH solution followed by  
133 incubation at  $37^\circ\text{C}$  for 1.5 h. After 1.5 h of incubation 10  $\mu\text{L}$  of a 100 $\mu\text{M}$  PAPS solution were added  
134 and the incubation continued under the same conditions for 1.5 h. The negative controls with either no  
135 analyte or no HLM were incubated as described above to exclude all the non-enzymatic reactions. Each  
136 specific incubation was performed in duplicate. The reaction was quenched with 100  $\mu\text{L}$  of acetonitrile  
137 ice cold, followed by centrifugation at 10000 rpm for 10 min (Centrifuge 5418, Eppendorf). The  
138 supernatant was removed and transferred to a new eppendorf tube and gently dried down by a stream  
139 of nitrogen at  $40^\circ\text{C}$  using TurboVap evaporator (Caliper, UK). The resulting residue was reconstituted  
140 with 50  $\mu\text{L}$  of a 80:20  $\text{H}_2\text{O}$ :MeOH solution containing the internal standard (100 ng/mL) and  
141 transferred into a polypropylene vial for analysis.

142 All analyses were undertaken using a Dionex Ultimate 3000 HPLC (Thermo Fisher UK Ltd.) coupled  
143 with a Bruker Maxis HD Q-TOF (Bruker) equipped with an electrospray ionization source. Nitrogen  
144 was used as nebulising gas at a flow rate of 11 L/min at a temperature of  $220^\circ\text{C}$  and at a pressure of 3  
145 Bar. Capillary voltage was set at 4500 V and End Plate offset was set at 500 V. The analyses were  
146 performed in both positive and negative modes and acquisition was performed in both full scan mode  
147 (MS) and broadband CID acquisition mode (MS/MS). HyStar™ Bruker was used to coordinate the LC-  
148 MS system. Chromatographic separation of the metabolites formed was achieved by using a WATERS  
149 ACQUITY UPLC BEH C18 column (50 mm x 2.1 mm, 1.7  $\mu\text{m}$ ) and the following mobile phase  
150 composition: 1 mM ammonium fluoride in water (A) and methanol (B). The gradient elution both in

151 ESI positive and negative mode was as follows: 5% B (0 -3 min) - 60% B (3 - 4 min) - 60% B (4 -14  
152 min), - 98% B (14 - 17 min) - 5% (17.1 - 20 min). The flow rate was kept constant at 0.4 ml/min and  
153 the column temperature was set at 40 °C. The source and operating parameters were optimized as  
154 follows: capillary voltage, 4500 V; dry gas temperature, 220 °C (N<sub>2</sub>); dry gas flow 12 L h<sup>-1</sup> (N<sub>2</sub>);  
155 quadrupole collision energy, 4 eV; collision energy, 7 eV MS (full-scan analysis) and 20 eV MS/MS  
156 (bbCID mode). Nitrogen was used as the nebulising, desolvation and collision gas. The method was  
157 fully quantitatively validated for PCMC (intra-day, accuracy 120.2%, precision 2.4%; inter-day,  
158 accuracy 120.2%, precision 3.5%; IQL, 22 ng/L; IDL, 6.6 ng/L; linearity range, 0.07-27.5 mg/mL; R<sup>2</sup>  
159 0.9987; MDL, 0.013 ng/L; MQL, 0.045 ng/L).

160 ***In vitro combined HLM/S9 fraction assay for verification of metabolic profile of PCMC*** Two  
161 incubation mixtures were prepared in duplicate by mixing 10 µL of phosphate buffer (50mM KH<sub>2</sub>PO<sub>4</sub>,  
162 pH 7.4, 5mM MgCl<sub>2</sub>), 10 µL of analyte solution (50µM), 10 µL of the 100µM UDPGA solution and 10  
163 µL of HLM spiked with 1 µL of an alamethicin solution 12.5 mg/mL. The reaction was initiated by  
164 addition of 10 µL of a 10 mM NADPH solution followed by incubation at 37°C. The incubation was  
165 carried out for 3 h under the same conditions for three of the four samples. At 3 h 10 µL of S9 fraction  
166 and 10 µL the 100µM PAPS solution were added to the samples to be incubated for six h and incubation  
167 was continued. The negative controls with either no analyte or no enzymes were prepared as well for  
168 each time point. After quenching the reaction with 100 µL of acetonitrile ice cold, samples were  
169 prepared for analysis as described above.

#### 170 ***In vivo pooled urine assay***

171 Seven pooled urine samples were collected from a UK festival event. They came from five different  
172 urinals sampled on three different days. Solid phase extraction (SPE) was performed on pooled urine  
173 samples using HLB Oasis® cartridges Water, UK) to reduce the matrix effect and to concentrate each  
174 sample by 4-fold. SPE procedure was as follows: 2 mL of pooled urine were loaded onto Oasis HLB  
175 cartridges, which were preconditioned with 2 mL MeOH followed by 2 mL H<sub>2</sub>O. After loading, the  
176 cartridges were dried for 30 min and analytes were eluted with 4 mL MeOH. Extracts were then dried  
177 under a gentle nitrogen stream using a TurboVap evaporator (Caliper, UK, 40°C). Dry extract was then  
178 reconstituted in 500 µL 80:20 H<sub>2</sub>O:MeOH, transferred to polypropylene vials and analysed using  
179 Dionex Ultimate 3000 HPLC coupled with a Bruker Maxis HD Q-TOF according to the procedure  
180 described above.

#### 181 ***Wastewater fingerprinting assay***

182 Raw wastewater samples collected from local wastewater treatment works, were filtered using GF/F  
183 glass microfibre filter 0.75 µm (Fisher Scientific, UK) followed by a solid phase extraction (SPE) using  
184 HLB Oasis® cartridges Water, UK) to reduce the matrix effect and to concentrate each sample by 400-  
185 fold. SPE procedure was as follows: 100 mL of filtered wastewater were loaded onto Oasis HLB  
186 cartridges, which were preconditioned with 2 mL MeOH followed by 2 mL H<sub>2</sub>O. After loading, the  
187 cartridges were dried for 30 min and analytes were eluted with 4 mL MeOH. Extracts were then dried  
188 under a gentle nitrogen stream using a TurboVap evaporator (Caliper, UK, 40°C). Dry extract was then  
189 reconstituted in 250 µL 80:20 H<sub>2</sub>O:MeOH, transferred to polypropylene vials and analysed using  
190 Dionex Ultimate 3000 HPLC coupled with a Bruker Maxis HD Q-TOF according to the procedure  
191 described above.

192 After analysis, data extracted from the Bruker system were processed with MetID software (Advanced  
193 Chemistry Development, Inc., ACD/Labs, UK) in order to predict metabolite structures. However, the  
194 software predicts a large number of possible metabolites, of which a rather small number is actually  
195 observed in *in vitro* experiments. We therefore developed a systematic workflow as presented in Figure  
196 1 to limit false positive measurements.

197

198

199

## 200 Results and discussion

### 201 *In vitro* assays

202 The *in vitro* metabolism of PCMC catalysed by CYP and SULT enzymes has been investigated using  
203 a combination of pooled HLM and S9 fraction tests. Hydroxylation of un-substituted carbon atoms was  
204 expected to be the major biotransformation reaction catalysed by CYPs whilst conjugations with phase  
205 II cofactors were expected to be the major reactions catalysed by UGT and ST. Phase II conjugations  
206 were expected to occur directly or following mono- and/or di-hydroxylation phase-I biotransformations.

207 ***In vitro HLM assay.*** After incubating PCMC with HLM a number of peaks were detected using LCMS.  
208 Initial analysis of samples, performed using ACDLabs software, identified two potential metabolites.  
209 A representative extracted ion chromatogram (XIC) of PCMC metabolites detected are reported in Figs.  
210 S1 and S2. All samples were analysed in negative and in positive ionisation modes. However, all the  
211 potential metabolites had better intensity in the negative ionization mode.

212 Incubation of PCMC produced a metabolite ( $m/z$  157.0057) with elemental composition of the  
213 deprotonated molecule denoting  $C_7H_6ClO^-$  (-3.6 ppm mass error) and a second one ( $m/z$  317.0422)  
214 with elemental composition of the deprotonated molecule denoting  $C_{13}H_{14}ClO_7^-$  (-3.8 ppm mass  
215 error). ACDLabs analysis led to their identification as mono-hydroxylated metabolite (Fig S1b) and  
216 glucuronide conjugated (Fig. S2b). PCMC hydroxylate did not provide a distinctive fragmentation  
217 pattern in bbCID mode which necessitated MS/MS analysis. Fragmentation of ions with  $m/z$  157.0062  
218  $\pm$  0.005 at 31 eV led to the formation of a fragment 121.0284 which corresponded with the loss of a  
219 chlorine moiety from the precursor ion (Fig. S1c). PCMC glucuronate instead produced in bbCID mode  
220 a fragment ion at  $m/z$  141.0108 ( $C_7H_6ClO^-$ , + 3.5 ppm mass error) that was assigned to  $[C_6H_8O_6]$  loss,  
221 and was related to the presence of a glucuronate group (Fig. S2c, bottom). The fragments obtained  
222 confirmed the chemical structure of the metabolites. Additionally, two chlorine isotope peaks at  $m/z$   
223 158.0086 and  $m/z$  159.0024 (Fig. S1d) and at  $m/z$  318.0452 and  $m/z$  319.0390 (Fig. S2d) were observed.  
224 The peaks had small mass errors (<5 ppm) and their relative heights match those expected from a  
225 compound with one chlorine within 5% of the predicted abundance.

226 PCMC metabolites have not been previously documented in literature, therefore the results of this study  
227 are of considerable importance. However, sulphate metabolites that were initially thought to be suitable  
228 as a biomarker were not detected in the *in-vitro* HLM assay. This could be due to two main factors.  
229 Firstly, the incubation time may not have been sufficiently long to allow detectable amounts of  
230 metabolites to be formed, as well as also not allowing the higher number of metabolites to be produced.  
231 Secondly this could be due to the lack of phase II enzymes being used such as sulphotransferases, of  
232 which HLM are deficient. To account for this, HLM/S9 fraction assay was undertaken (see below).

233 ***In vitro combined HLM/S9 fraction assay.*** The *in vitro* combined HLM/S9 fraction assay included  
234 verification of quantitative and qualitative changes of metabolic profile in two time intervals (3 and 6  
235 h). Moreover, due to the addition of the S9 fraction to the incubation mixture, further metabolites  
236 (sulphate conjugated) were expected to be produced. Indeed, an incubation of PCMC with pooled  
237 HLM/S9 fraction produced two further metabolites: sulphated PCMC and mono-hydroxylated  
238 sulphated PCMC (Fig. 2 and S3).

239 It can be seen in Fig. 2 that the *in vitro* test leads to the formation of a metabolite with retention time  
240 denoting 6.4 min (Fig. 2b, dark peak). This chromatographic peak was absent in the blank control (Fig.  
241 2a). Spectral analysis performed using ACDLabs software identified the compound to be a sulphated  
242 metabolite ( $m/z$  220.9684). Elemental composition of the deprotonated molecule of the sulphated  
243 metabolite was assigned as  $C_7H_6ClO_4S^-$  (+ 1.3 ppm mass error). The fragment ion at  $m/z$  141.0117  
244 ( $C_7H_6ClO^-$ , + 3.6 ppm mass error) was assigned to  $[O_3S]$  loss, and was related to the presence of a  
245 sulphate group (Fig. 2c, bottom). To further confirm that the fragment ion originates from the suspected  
246 metabolite its chromatogram was extracted. The resulting XIC produced a peak whose elution time  
247 matched perfectly with that of the suspected metabolite (Fig. 2b, light peak). Additionally, the presence  
248 of two chlorine isotope peaks at  $m/z$  221.9713 and  $m/z$  222.9653 (Fig. 2d) was observed. The peaks

249 had small mass errors <5 ppm and their relative heights match those expected from a compound with  
250 one chlorine within 5% of the predicted abundance.

251 The *in vitro* HLM/S9 fraction assay led to the formation of another PCMC metabolite with retention  
252 time of 6.3 min (Fig S3b, dark peak). This is the same chromatographic peak that was absent in the  
253 blank control (Fig. S3a). Spectral analysis performed using ACDLabs software identified the compound  
254 to be the sulphated and hydroxylated metabolite (m/z 236.9632). Elemental composition of the  
255 deprotonated molecule of the metabolite was assigned as C<sub>7</sub>H<sub>6</sub>ClO<sub>5</sub>S<sup>-</sup> (+ 1.3 ppm mass error). The  
256 fragment ion at m/z 157.0065 (C<sub>7</sub>H<sub>6</sub>ClO<sub>2</sub><sup>-</sup>, + 1.9 ppm mass error) was assigned to [O<sub>3</sub>S] loss, and was  
257 related, as previously, to the presence of a sulphate group (Fig. S3c, bottom). To further confirm that  
258 the fragment ion originates from the suspected metabolite its chromatogram was extracted. The  
259 resulting XIC produced a peak whose elution time matched perfectly with that of the suspected  
260 metabolite (Fig. S3b, light peak). Also, as above, two chlorine isotope peaks at m/z 237.9664 and m/z  
261 238.9601 (Fig. S3d) were observed. The peaks had small mass errors <5 ppm and their relative heights  
262 matched those expected from a compound with one chlorine within 5% of the predicted abundance.

263 Phase II cofactor (PAPS) was added after 3 h to the incubation mixture to permit all the possible phase  
264 I metabolites to form before conjugation with sulphate took place. This approach attempts to replicate  
265 what happens in a living cell, where generally (but not necessarily) phase I minor biotransformations  
266 occur in preparation for successive phase II conjugation. Results are summarised in Fig. S4. It can be  
267 seen from Fig. S4 that hydroxylated metabolites are preferentially formed after 3 h of incubation time  
268 (88.7% against 11.3% conjugation with glucuronic acid). The hydroxylated PCMC was still the most  
269 abundant biotransformation product (40% of the total metabolites produced circa) after 6 h of incubation  
270 time, although at this sampling point phase II metabolites accounted for 59.8% of all the metabolites  
271 produced. In particular amongst the three phase II biotransformation observed after 6 h direct sulphation  
272 seemed to be the preferential conjugation route accounting for more than 25% of total  
273 biotransformation.

274 In summary, both HLM and HLM-S9 fraction assays allowed for the identification of metabolites that  
275 have not been previously documented in literature, although the latter assay allowed the identification  
276 of a higher number of metabolites due to the addition of the S9 fraction resulting in a more efficient  
277 sulphation. Moreover a two-step approach, which entails the addition of phase II enzymes and  
278 sulphation cofactor after 3 h permits the identification of all the phase I and II metabolites and  
279 conjugated metabolites, providing a wider range of biotransformation products. The formation of  
280 PCMC sulphate conjugates means also that a more efficient sulphate conjugation takes place in the  
281 HLM-S9 fraction assay, when compared to the HLM assay. All the identified metabolites are presented  
282 in Tab. 1. The table reports also elemental composition and the mass accuracy measured in the two *in*  
283 *vitro* assays and in a wastewater sample from a local wastewater treatment plant (WWTP) (see  
284 discussion below).

#### 285 ***In vivo pooled urine assay***

286 The *in vivo* pooled urine assay led to identification of only one metabolite of PCMC, sulphated PCMC  
287 (Tab. 1 and Fig. 3). Interestingly, hydroxylated and glucuronated metabolites were not observed in  
288 analysed pooled urine samples. This is in contrast with *in vitro* assays where glucuronated, sulphated  
289 and hydroxylated metabolites were identified.

#### 290 ***In vivo wastewater fingerprinting assay***

291 The aim of the two *in vitro* assays was to select potential biomarkers of exposure to PCMC. However,  
292 as the ultimate goal of this study was to verify community-wide exposure to these chemicals, analysis  
293 of untreated wastewater samples serving large community of 70 thousand people was undertaken. The  
294 identification of biomarkers was based on the systematic workflow presented in Fig. 1. The compounds  
295 detected in wastewater are summarised in Tab. 1. As expected, given the complexity of the matrix,  
296 mass accuracy measured was lower than that measured in *in vitro* studies but still within set limits, with  
297 mass error values between 5 and 10 ppm (Tab. 1).

298 In vivo wastewater fingerprinting assay resulted in the detection and identification of only one  
299 metabolite of PCMC, sulphated PCMC, in wastewater (Fig. 4). The loss of [O<sub>3</sub>S] deduced by TOF MS  
300 spectra has been crucial for justifying and suggesting possible chemical structures. Interestingly,  
301 hydroxylated and glucuronated PCMC were not observed in analysed wastewater samples. This is in  
302 line with results obtained for *in vivo* pooled urine assay and it confirms that *in vitro* studies, although  
303 informative, cannot serve as the only tool intended for selection of biomarkers of exposure.

## 304 **Conclusions**

305 This study proved that combined human metabolism and wastewater fingerprinting assay is a powerful  
306 tool to investigate human exposure to chemicals present in personal care products and a wider-group of  
307 chemicals that are not intended for human consumption and therefore lack comprehensive risk  
308 assessment data. We have proposed a robust systematic workflow that enables fast and comprehensive  
309 selection of characteristic biomarkers of public exposure to chemical substances (Fig. 1). The workflow  
310 consists of several steps: Step 1: *In vitro* HLM/S9 assay; Step 2: *In vivo* pooled urine assay; Step 3: *In*  
311 *in vivo* wastewater fingerprinting assay; Step 4: Analysis with HR-MSMS; Step 5: Data processing and  
312 Step 6: Selection of biomarkers. In Step 4, after the establishment of a list of suspected metabolites  
313 using ACDLab software (Step 4a), in order to avoid false positives, their accurate mass, retention time  
314 and fragmentation pattern are examined (Step 4b,c,d). Finally the structure of the suspects is confirmed  
315 by investigating the MS/MS fragmentation pattern in *bbCID* mode (Step 4e). For those metabolites that  
316 do not provide an optimal MS/MS fragmentation pattern in *bbCID* mode, a further confirmation step  
317 performing a data-dependent MS/MS acquisition is required (Step 4f), i.e. an MS/MS analysis is  
318 triggered if a compound from a target ion list is detected. In contrast to targeted screening, non-target  
319 screening starts without any a priori information on the compounds to be detected. However, this study  
320 falls in between these two categories, since the chemically meaningful structures which can be assigned  
321 to an unknown peak are limited to structures showing a close relationship with the parent compound.

322 Four new possible metabolites of PCMC (hydroxylated, glucuronidated, sulphated and hydroxylated &  
323 sulphated PCMC) were identified after *in vitro* HLM/S9 studies and were proposed as biomarkers of  
324 exposure. The absence of phase I metabolites in the presence of phase II cofactor PAPS suggested that  
325 sulphation was the preferential metabolic pathway for this compound. Only one of these metabolites  
326 (PCMC sulphated) was confirmed in wastewater and in urine suggesting human internal exposure to  
327 PCMC despite the fact that this compound is utilised in products meant for external use. Consequently  
328 to the results obtained in this present work it seems evident that the impact of the exposure to PCMC  
329 and other chemicals not intended for human consumption might need to be reconsidered. Also in a  
330 realistic overview of its impact on the aquatic ecosystem its identified metabolite should be also  
331 investigated to verify their potential environmental impact.

332 The aim of this paper was to introduce a new assay for identification of new metabolic biomarkers in  
333 WBE. Further work will be undertaken to verify utility of selected biomarkers in a large urban water  
334 catchment monitoring campaign.

## 335 **ACKNOWLEDGMENTS**

336 The support of the Leverhulme Trust (Project No RPG-2013-297) is greatly appreciated. We would  
337 also like to acknowledge TICTAC Communications (St George's University of London, United  
338 Kingdom) for provision of pooled urine samples. All data supporting this study are provided as  
339 supporting information accompanying this paper.

340

341

342

343

344

345



346 **ASSOCIATED CONTENT**

347 The Supporting Information is available free of charge on the ACS Publications website

348 Supporting Information includes the following:

349 Figure S1 XIC of hydroxylated PCMC metabolite produced with HLM. XICs at m/z 157.0062 (0.005-  
350 Da mass-window width) for analyte-sample (b), blank control (a), fragmentation pattern of the  
351 metabolite obtained in MRM mode (c) and XIC at m/z 157.0049, 158.0079 and 159.0017 for PCMC  
352 and the two chlorine isotope peaks (top), and mass spectra (bottom).

353 Figure S2 Detection and identification of PCMC glucuronate metabolite by UHPLC-QTOF-MS  
354 following in-vitro HLM assay (3 hour time point). XICs at m/z 307.0646 and 227.1078 (0.005-Da mass-  
355 window width) for analyte-sample (b) and control-sample (a). (c) (top) Low-energy (full-scan analysis)  
356 and (bottom) high-energy (bbCID mode) spectra of the metabolite and fragment ion observed. (d) XIC  
357 at m/z 317.0422, 318.0452 and 319.0390 for PCMC glucuronate and the two chlorine isotope peaks  
358 (top), and mass spectra (bottom).

359 Figure S3 Detection and identification of sulphated and hydroxylated PCMC by UHPLC-QTOF-MS  
360 following in-vitro HLM/S9 assay. XICs at m/z 236.9630 and 157.0062 (0.005-Da mass-window width)  
361 for analyte-sample (b) and control-sample (a). (c) (top) Low-energy (full-scan analysis) and (bottom)  
362 high-energy (bbCID mode) spectra and structures of the metabolite and fragment ion observed. (d) XIC  
363 at m/z 236.9632, 237.9660 and 238.9601 for PCMC hydroxylate & sulphate and the two chlorine  
364 isotope peaks (top) and mass spectra (bottom).

365 Figure S4 Distribution of PCMC metabolites obtained with in-vitro HLM and HLM/S9 fraction assay  
366 over a 3 and 6 h incubation time.

367 Report 1 Detection and identification of PCMC metabolites by UHPLC-QTOF-MS following *in-vitro*  
368 HLM assay.

- 369
- 370 • Sample Name 4-Cl-3-Me\_1\_neg and PCMC\_10ul\_enz\_B\_Neg\_2 XIC and mass spectrum of  
371 PCMC hydroxylated, PCMC glucuronidated, PCMC and relative isotopes following *in-vitro*  
372 HLM assay for verification of metabolic profile of PCMC.
  - 373 • Sample Name 4-Cl-3-Me\_2\_neg and PCMC\_10ul\_enz\_B\_Neg\_2 XIC and mass spectrum of  
374 PCMC hydroxylated, PCMC glucuronidated, PCMC and relative isotopes following *in-vitro*  
375 HLM assay for verification of metabolic profile of PCMC (duplicate sample)
  - 376 • Sample Name 4-Cl-3-Me\_Blank\_neg and PCMC\_blank\_Neg XIC and mass spectrum of  
377 PCMC hydroxylated, PCMC glucuronidated, PCMC and relative isotopes following *in-vitro*  
378 HLM assay for verification of metabolic profile of PCMC (blank control)

379 Report 2 Detection and identification of PCMC metabolites by UHPLC-QTOF-MS following *in-vitro*  
380 HLM/S9 assay.

- 381
- 382 • Sample Name S9\_4-Cl-3-Me\_A\_6\_Hour\_Neg and 4\_Cl\_6hA\_Neg XIC and mass spectrum of  
383 PCMC hydroxylated, PCMC glucuronidated, PCMC sulfated, PCMC sulfated and  
384 hydroxylated, PCMC and relative isotopes (including bbCID fragmentation pattern for phase  
385 II metabolites), following *in-vitro* HLM/S9 assay (6 hour sampling point) for verification of  
386 metabolic profile of PCMC.
  - 387 • Sample Name S9\_4-Cl-3-Me\_B\_6\_Hour\_Neg and 4\_Cl\_6hB\_Neg XIC and mass spectrum of  
388 PCMC hydroxylated, PCMC glucuronidated, PCMC sulfated, PCMC sulfated and  
389 hydroxylated, PCMC and relative isotopes (including bbCID fragmentation pattern for phase  
390 II metabolites), following *in-vitro* HLM/S9 assay (6 hour sampling point) for verification of  
391 metabolic profile of PCMC. (duplicate sample)
  - 392 • Sample Name S9\_4-Cl-3-Me\_Blank\_6\_Hour\_Neg and 4\_Cl\_6hBlank\_Neg XIC and mass  
393 spectrum of PCMC hydroxylated, PCMC glucuronidated, PCMC sulfated, PCMC sulfated and  
394 hydroxylated, PCMC and relative isotopes (including bbCID fragmentation pattern for phase

393 II metabolites), following *in-vitro* HLM/S9 assay (6 hour sampling point) for verification of  
394 metabolic profile of PCMC. (blank control)

395 Report 3 Detection and identification of PCMC metabolite by UHPLC-QTOF-MS following urine  
396 analysis.

397 • Sample Name Urine\_141\_A neg XIC and mass spectrum of PCMC sulfated (including bbCID  
398 fragmentation pattern) and relative isotopes, following direct *in-vivo* urine profiling assay.

399 • Sample Name Urine\_141\_B neg XIC and mass spectrum of PCMC sulfated (including bbCID  
400 fragmentation pattern) and relative isotopes, following direct *in-vivo* urine profiling assay.

401 Report 4 Detection and identification of PCMC metabolites by UHPLC-QTOF-MS following  
402 wastewater analysis.

403 • Sample Name Inf day 1A neg XIC and mass spectrum of PCMC and PCMC sulphated  
404 (including bbCID fragmentation pattern) and relative isotopes.

405 Report 5 MRM fragmentation pattern of PCMC standard solution.

406 • Sample Name MRM\_4Cl3MPox\_Met2\_STD\_5 MRM fragmentation pattern of PCMC  
407 standard solution

## 408 References

409 (1) Aiello, A. E.; Larson, E. L.; Levy, S. B. *Clin. Infect. Dis.* **2007**, *45 Suppl 2*, S137–S147.

410 (2) Dhillon, G. S.; Kaur, S.; Pulicharla, R.; Brar, S. K.; Cledón, M.; Verma, M.; Surampalli, R. Y. *Int. J.*  
411 *Environ. Res. Public Health* **2015**, *12* (5), 5657–5684.

412 (3) Ahn, K. C.; Zhao, B.; Chen, J.; Cherednichenko, G.; Sanmarti, E.; Denison, M. S.; Lasley, B.;  
413 Pessah, I. N.; Kültz, D.; Chang, D. P. Y.; Gee, S. J.; Hammock, B. D. *Environ. Health Perspect.*  
414 **2008**, *116* (9), 1203–1210.

415 (4) Rostkowski, P.; Horwood, J.; Shears, J. A.; Lange, A.; Oladapo, F. O.; Besselink, H. T.; Tyler, C. R.;  
416 Hill, E. M. *Environ. Sci. Technol.* **2011**, *45* (24), 10660–10667.

417 (5) Gautam, P.; Carsella, J. S.; Kinney, C. A. *Water Res.* **2014**, *48* (1), 247–256.

418 (6) Aiello, A. E.; Marshall, B.; Levy, S. B.; Della-Latta, P.; Lin, S. X.; Larson, E. *Emerg. Infect. Dis.* **2005**,  
419 *11* (10), 1565–1570.

420 (7) Moss, T.; Howes, D.; Williams, F. M. *Food Chem. Toxicol.* **2000**, *38* (4), 361–370.

421 (8) Loraine, G. a.; Pettigrove, M. E. *Environ. Sci. Technol* **2006**, *40* (3), 687–695.

422 (9) Wu, X.; Ernst, F.; Conkle, J. L.; Gan, J. *Environ. Int.* **2013**, *60*, 15–22.

423 (10) Geens, T.; Roosens, L.; Neels, H.; Covaci, A. *Chemosphere* **2009**, *76* (6), 755–760.

424 (11) Allmyr, M.; Harden, F.; Toms, L. M. L.; Mueller, J. F.; McLachlan, M. S.; Adolfsson-Erici, M.;  
425 Sandborgh-Englund, G. *Sci. Total Environ.* **2008**, *393* (1), 162–167.

426 (12) Heffernan, A. L.; Baduel, C.; Toms, L. M. L.; Calafat, A. M.; Ye, X.; Hobson, P.; Broomhall, S.;  
427 Mueller, J. F. *Environ. Int.* **2015**, *85*, 77–83.

428 (13) Asimakopoulos, A. G.; Thomaidis, N. S.; Kannan, K. *Sci. Total Environ.* **2014**, *470*, 1243–1249.

429 (14) Ye, X.; Zhou, X.; Furr, J.; Ahn, K. C.; Hammock, B. D.; Gray, E. L.; Calafat, A. M. *Toxicology* **2011**,  
430 *286* (1-3), 69–74.

431 (15) Wu, J.; Liu, J.; Cai, Z. **2010**, 1828–1834.

432 (16) Kumar, B.; Verma, V. K.; Sharma, C. S.; Akolkar, A. B. *J. Xenobiotics* **2014**, *4* (1), 46–52.

- 433 (17) Coogan, M. a; La Point, T. W. *Environ. Toxicol. Chem.* **2008**, 27 (8), 1788–1793.
- 434 (18) Yazdankhah, S. P.; Scheie, A. a; Høiby, E. A.; Lunestad, B.-T.; Heir, E.; Fotland, T. Ø.; Naterstad,  
435 K.; Kruse, H. *Microb. Drug Resist.* **2006**, 12 (2), 83–90.
- 436 (19) Silins, I.; Högberg, J. *Int. J. Environ. Res. Public Health* **2011**, 8 (3), 629–647.
- 437 (20) Chen, C.; Kostakis, C.; Gerber, J. P.; Tschärke, B. J.; Irvine, R. J.; White, J. M. *Sci. Total Environ.*  
438 **2014**, 487, 621–628.
- 439 (21) Daughton, C. G. *Sci. Total Environ.* **2012**, 414, 6–21.
- 440 (22) Baker, D. R.; Barron, L.; Kasprzyk-Hordern, B. *Sci. Total Environ.* **2014**, 487 (1), 629–641.
- 441 (23) Yang, Z.; Castrignanò, E.; Estrela, P.; Frost, C. G.; Kasprzyk-Hordern, B. *Sci. Rep.* **2016**, 6 (October  
442 2015), 21024.
- 443 (24) Reid, M. J.; Thomas, K. V. *Environ. Sci. Technol.* **2011**, 45 (18), 7611–7612.
- 444 (25) Schebb, N. H.; Inceoglu, B.; Ahn, K. C.; Morisseau, C.; Gee, S. J.; Hammock, B. D. **2011**, 3109–  
445 3115.
- 446 (26) Miller, D.; Wheals, B. B.; Beresford, N.; Sumpter, J. P. *Environ. Health Perspect.* **2001**, 109 (2),  
447 133–138.
- 448 (27) Ortopedico, O.; San, D. H.; Scientific, R. .
- 449 (28) Ghisari, M.; Bonefeld-Jorgensen, E. C. *Toxicol. Lett.* **2009**, 189 (1), 67–77.
- 450 (29) Ballesteros-Gómez, A.; Erratico, C. a; Eede, N. Van Den; Ionas, A. C.; Leonards, P. E. G.; Covaci,  
451 A. *Toxicol. Lett.* **2014**, 232 (1), 203–212.
- 452 (30) Brandon, E. F. a; Raap, C. D.; Meijerman, I.; Beijnen, J. H.; Schellens, J. H. M. *Toxicol. Appl.*  
453 *Pharmacol.* **2003**, 189 (3), 233–246.
- 454

455 Table 1 PCMC and their metabolic biomarkers.

Compound	Elemental composition [M-H] <sup>-</sup>	Exact mass (m/z)	<i>In-vitro</i> HLM assay		<i>In-vitro</i> HLM/S9 fraction assay		<i>In-vivo</i> pooled urine assay		<i>In-vivo</i> wastewater fingerprinting assay	
			Peak top mass (m/z)	Mass error (ppm)	Peak top mass (m/z)	Mass error (ppm)	Peak top mass (m/z)	Mass error (ppm)	Peak top mass (m/z)	Mass error (ppm)
PCMC	C <sub>7</sub> H <sub>6</sub> ClO <sup>-</sup>	141.0113	141.0118	+3.6	141.0116	+2.1	-	-	141.0122	+6.0
PCMC hydroxylated	C <sub>7</sub> H <sub>6</sub> ClO <sub>2</sub> <sup>-</sup>	157.0062	157.0049	-8.2	157.0061	-0.6	-	-	-	-
PCMC glucuronidated	C <sub>13</sub> H <sub>15</sub> ClO <sub>7</sub> <sup>-</sup>	317.0434	317.0422	-3.8	317.0442	+2.5	-	-	-	-
PCMC sulphated	C <sub>7</sub> H <sub>6</sub> ClO <sub>4</sub> S <sup>-</sup>	220.9681	-	-	220.9684	+1.3	220.9670	- 5	220.9695	+6.4
PCMC hydroxylated & sulphated	C <sub>7</sub> H <sub>6</sub> ClO <sub>5</sub> S <sup>-</sup>	236.9630	-	-	236.9632	+0.9	-	-	-	-

456

457

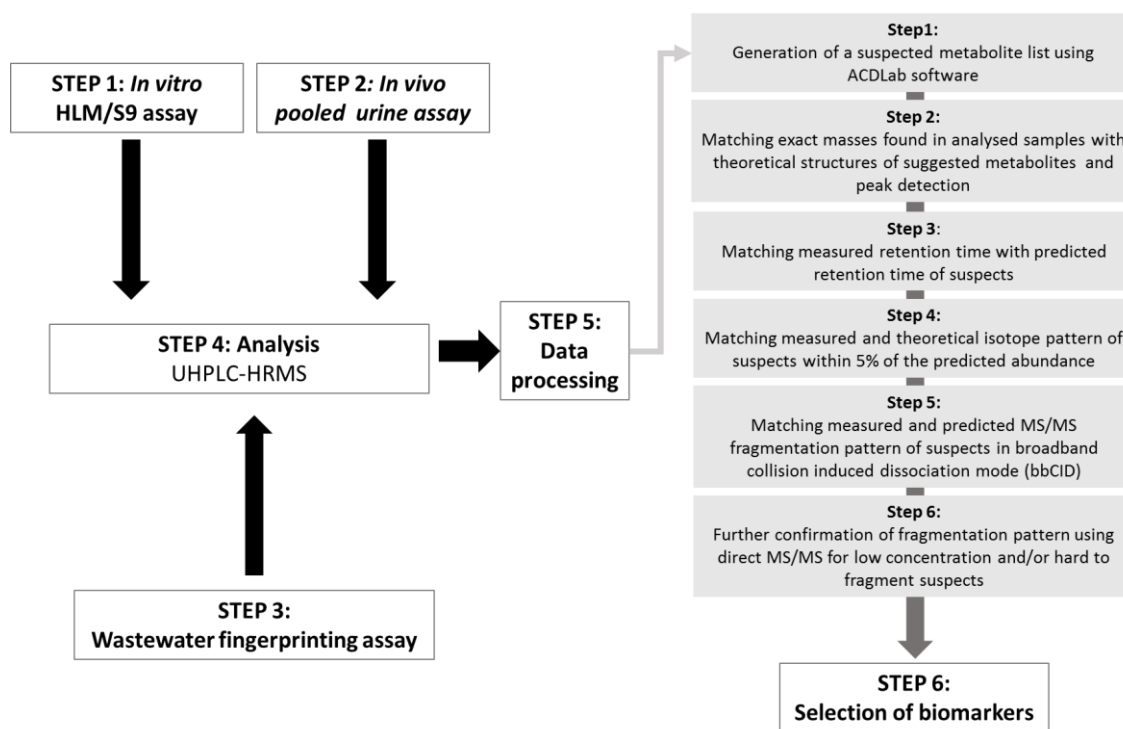


Figure 1 A systematic workflow for verifying human exposure to chemicals via combined *in-vitro* HLM/S9 and *in-vivo* pooled urine and wastewater profiling assay

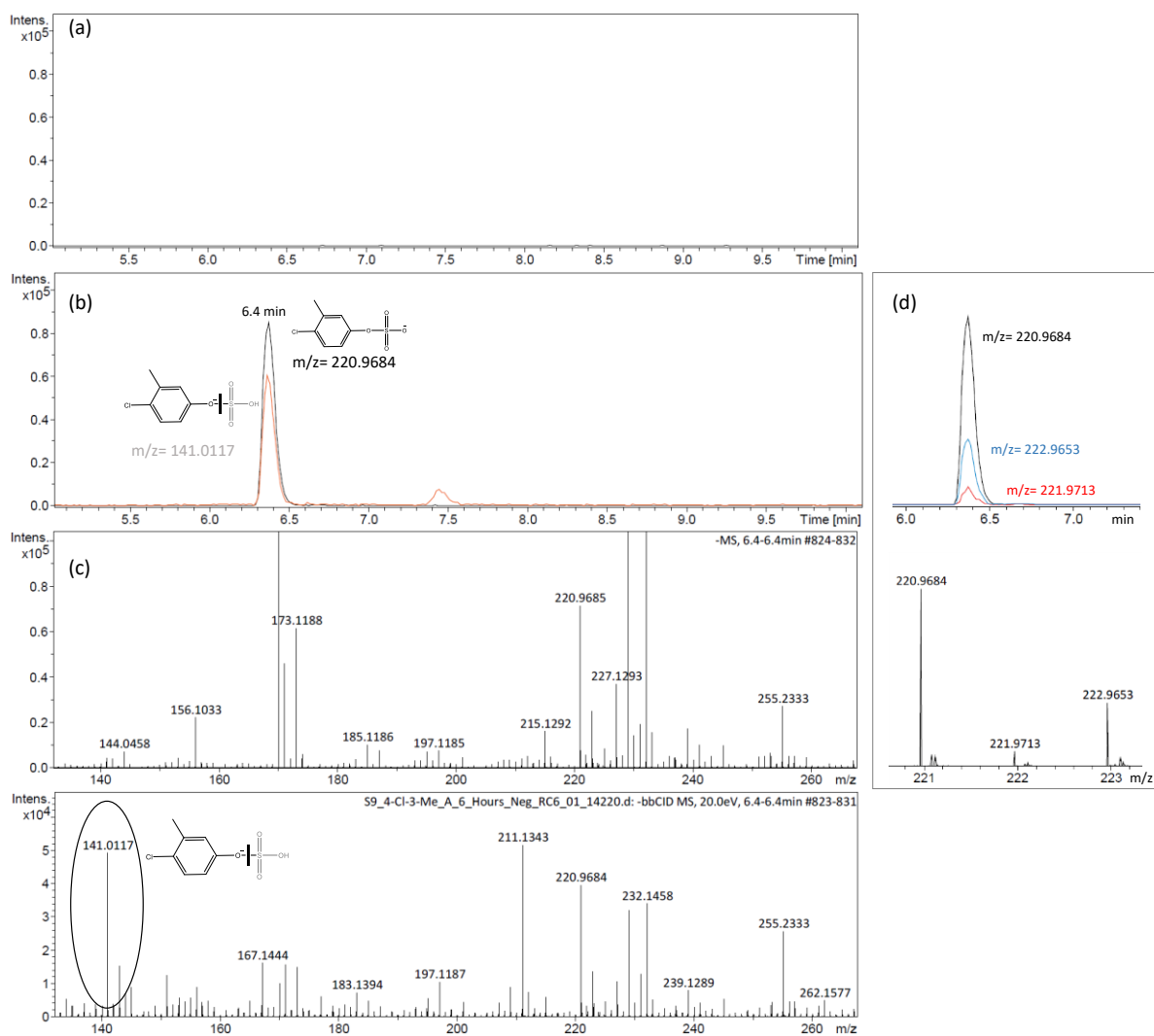


Figure 2 Detection and identification of sulphated PCMC by UHPLC-QTOF-MS following *in-vitro* HLM/S9 assay. XICs at  $m/z$  220.9681 and 141.0113 (0.005-Da mass-window width) for analyte-sample (b) and control-sample (a). (c) (top) Low-energy (full-scan analysis) and (bottom) high-energy (bbCID mode) spectra and structures of the metabolite and fragment ion observed. (d) XIC at  $m/z$  220.9684, 221.9713 and 222.9653 for PCMC sulphate and the two chlorine isotope peaks (top) and mass spectra (bottom).

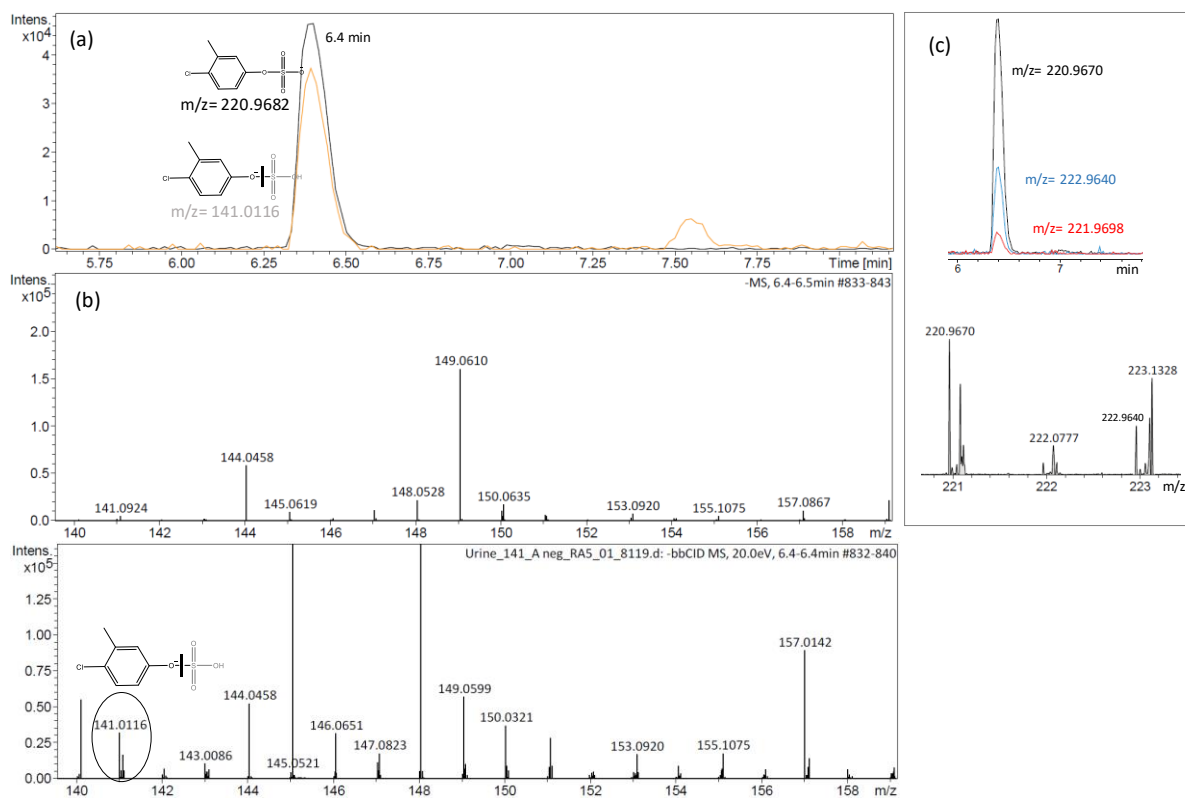


Figure 3 Detection and identification of sulphated PCMC by UHPLC-QTOF-MS following *in-vivo* poled urine assay. (a) XICs at  $m/z$  220.9681 and 141.0113 (0.005-Da mass-window width). (b) (top) Low-energy (full-scan analysis) and (bottom) high-energy (bbCID mode) spectra and structures of the metabolite and fragment ion observed. (c) XIC at  $m/z$  220.9670, 221.9698 and 222.9640 (0.005-Da mass-window width) for PCMC and the two chlorine isotope peaks (top) and mass spectra (bottom).

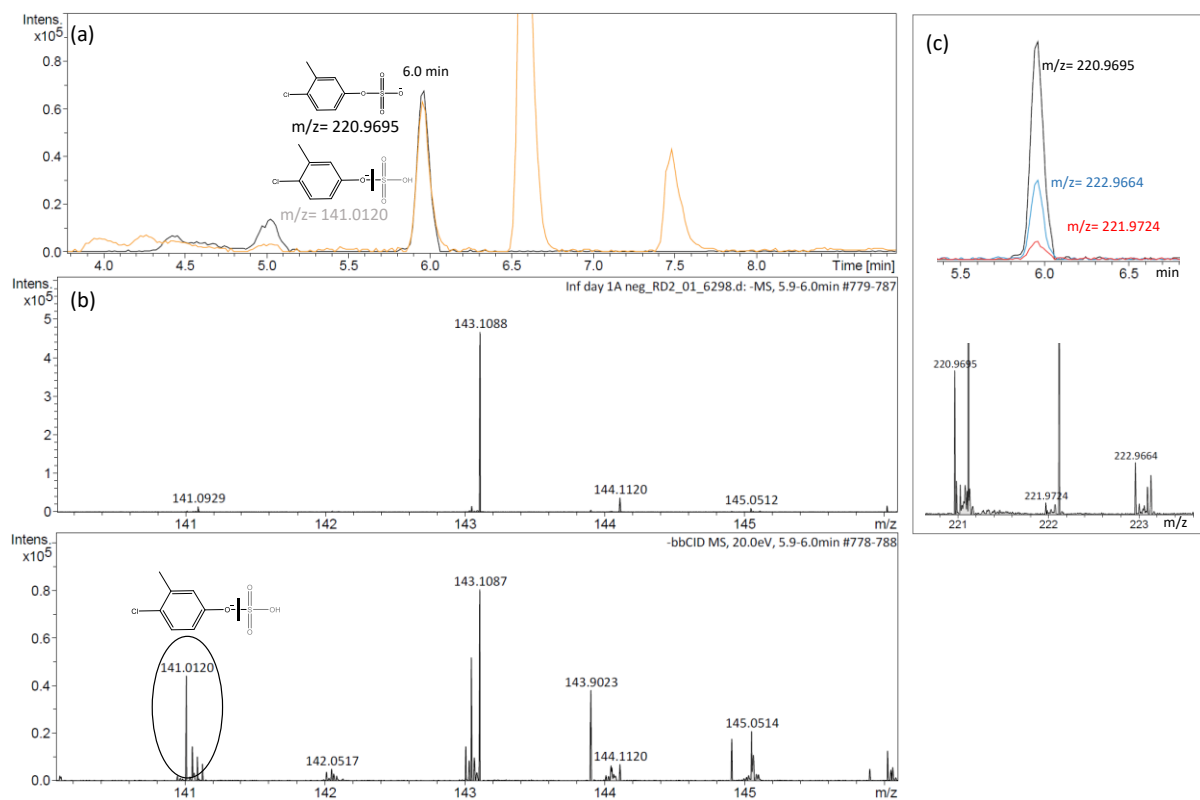


Figure 4 Detection and identification of sulphated PCMC by UHPLC-QTOF-MS following *in-vivo* wastewater profiling assay. (a) XICs at m/z 220.9681 and 141.0113 (0.005-Da mass-window width). (b) (top) Low-energy (full-scan analysis) and (bottom) high-energy (bbCID mode) spectra and structures of the metabolite and fragment ion observed. (c) XIC at m/z 220.9695, 221.9724 and 222.9664 (0.005-Da mass-window width) for PCMC and the two chlorine isotope peaks (top) and mass spectra (bottom).